

## Isoelectronic Trap Li-Li-O in GaP

P. J. Dean\*

*Bell Telephone Laboratories, Murray Hill, New Jersey 07974*

(Received 18 January 1971)

Strong red low-temperature photoluminescence results from Li diffusion of as-grown GaP crystals prepared from the vapor by the wet H<sub>2</sub> method, or from Ga solution with O doping. The luminescence spectrum contains sharp strong no-phonon lines and many well-resolved phonon replicas. Four no-phonon lines can be seen at zero field. The spacings between these lines are approximately consistent with a model in which the luminescence arises from the decay of an exciton bound by  $\sim 0.24$  eV to an axial ( $C_{3v}$ ) center. The  $J$ - $J$  and crystal-field splittings are 1.1 and 3.4 meV. The symmetry axis is shown to be  $\langle 111 \rangle$  from detailed magneto-optical studies of the no-phonon lines, and the electron and hole  $g$  values are determined from an analysis for strong crystal field,  $g_e = 1.76 \pm 0.14$ ,  $g_h = 1.04 \pm 0.05$ . Use of this form of analysis is suggested by the degree of mixing of the  $J$ - $J$ -split states by the crystal field, indicated by the relative oscillator strengths of the no-phonon lines. The chemical identity of components of this axial center has been determined from isotope experiments. The substitution  $O^{16} \rightarrow O^{18}$  increases the no-phonon line energies by 0.8 meV, and shifts some of the many local-mode lines resolved in the phonon wing of the luminescence spectrum. Only changes in local-mode energies occur for the substitution  $Li^7 \rightarrow Li^6$ , but these changes are generally larger than for O. The form of the true local-mode replicas for crystals containing roughly equal amounts of  $Li^6$  and  $Li^7$  proves that the center contains at least *two inequivalent* Li atoms. The simplest model for the center consistent with all the detailed experimental evidence is  $Li_I - Li_{Ca} - O_P$  ( $I$  = interstitial). This complex is isoelectronic with the Ga-P atom pair it replaces, can produce efficient low-temperature bound-exciton luminescence with decay time consistent with experiment ( $\sim 200$  nsec for decay allowed by electric dipole selection rules), and has no free spin in the final state. The temperature quenching rate of the Li-Li-O luminescence is large compared with the familiar red Zn-O luminescence because of the high degree of compensation produced by Li diffusion, and the Li-Li-O photo- and electroluminescence efficiencies are negligible near 300 °K. The associate  $V_{Ca} - O_P$  ( $V$  = vacancy) is necessary for the formation of the Li-Li-O centers. Evidence is presented that a significant proportion of the substitutional O exists in these associates before Li diffusion for GaP crystals grown or annealed below 1100 °C. Apparently, the  $V_{Ca} - O_P$  associate is not stable significantly above 1100 °C, while association is essentially quenched at  $T \lesssim 700$  °C. The behavior of  $V_{Ca}$  in GaP can be studied very conveniently from the optical properties of the Li-Li-O associate. In addition, the efficiency of O-doping techniques for GaP crystals grown by different methods can be assessed easily and with high accuracy and sensitivity by purely optical measurements, using appropriate annealing techniques together with  $O^{18}$  doping.

## I. INTRODUCTION

The importance of isoelectronic traps for the extrinsic optical properties of semiconductors was first clearly demonstrated in GaP, with the trap  $N$ .<sup>1</sup> Since then, further isoelectronic traps have been discovered both in GaP and in other semiconductors.<sup>2</sup> Most of these traps are point defects, involving a single impurity on a substitutional (lattice) site. Two well-authenticated cases of isoelectronic traps involving compound substitutions also occur in GaP, where nearest-neighbor pairs of GaP are replaced by ZnO or CdO, forming deep bound states for electrons.<sup>3,4</sup>

In the present paper, we describe a new isoelectronic trap in GaP, the complex  $Li_I - Li_{Ca} - O_P$  present in Li-diffused GaP. Here, the subscripts indicate whether the impurity atom substitutes for Ga or P, or is interstitial ( $I$ ). At low temperatures this center introduces efficient red luminescence

due to the recombination of excitons bound by  $\sim 240$  meV. The luminous equivalent of this red light is significantly higher than the red luminescence introduced by  $Zn_{Ca} - O_P$  associates, used in red GaP light-emitting diodes. Unfortunately, the temperature quenching rate of the Li-Li-O luminescence is much greater than for the Zn-O luminescence (Sec. III G), and the prospects for efficient room-temperature Li-Li-O red light are dim. The Li-Li-O trap is an example of a qualitatively new situation, in which a molecule of the host GaP is replaced isoelectronically by *three* atoms. The axial ( $\langle 111 \rangle$ ) symmetry of Li-Li-O in GaP, established from the Zeeman spectrum of the bound exciton (Sec. III C) indicates a linear configuration for  $Li_I - Li_{Ca} - O_P$ . The presence of *at least two* Li atoms on *inequivalent* sites (Ga and  $I$ ) is unambiguously established from the Li local modes seen in the phonon wing of the Li-Li-O luminescence spectrum (Secs. III A and III D). Just *two* Li atoms

are necessary and sufficient to make the Li-Li-O associate isoelectronic with GaP, thus providing a center which can trap an exciton with large binding energy and yet produce efficient luminescence at low temperatures with a moderately long lifetime (Sec. III E). The involvement of O in the electronic transition is proved beyond doubt by the observation of spectral changes when  $O^{16}$  is replaced by  $O^{18}$  (Secs. III A and III D). The atomic sequence in this linear associate is established from the condition of minimum electrostatic interaction energy for these donor and acceptor ions,<sup>5</sup> and is quite different from the free  $Li_2O$  molecule.<sup>6</sup>

Optical absorption of the Li-Li-O traps has also been seen (Sec. III D). The concentration of these traps can be calculated from absorption using the measured lifetime for bound-exciton transitions allowed by electric dipole selection rules. This concentration [Li-Li-O] is comparable with the concentration of optically active O donors present in these crystals before Li diffusion, suggesting that a large proportion of these O donors become paired with  $Li_2$  during the standard diffusion treatment. Comparison of the intensity of the red Li-Li-O luminescence after Li diffusion under standard conditions in GaP crystals grown by different methods, and subjected to different annealing treatments (Sec. III F), suggests that the presence of the complex  $V_{Ga}-O_p$  is a necessary prerequisite for the appearance of the Li-Li-O center. These studies suggest that a significant proportion of the substitutional O donors in GaP grown or annealed at  $\sim 1000^\circ C$  exists in the form of  $V_{Ga}-O_p$  associates prior to the Li diffusion. In the author's opinion, this is one of the most definitive pieces of evidence of the behavior of Ga vacancies in a III-V compound, and specifically for vacancy-donor pairing. Pairing of Ga vacancies and donors has been implicated in deep center luminescence in GaAs,<sup>7</sup> but the identifications are not unequivocal.

Other less dramatic spectral features occur in Li-diffused GaP. These will be the subject of a separate publication.

## II. EXPERIMENTAL

### A. Crystal Preparation

A variety of GaP crystals were used in these experiments. Some were grown at  $\sim 1470^\circ C$  from a stoichiometric GaP melt by the liquid-encapsulated Czochralski (LEC) technique.<sup>8</sup> The as-received crystals generally did not show the characteristic red luminescence of the Li-Li-O trap, even though many were deliberately O doped and were closely compensated by the Li diffusion. However, these O-doped LEC crystals did show strong Li-Li-O luminescence on diffusion with Li at  $700^\circ C$  after a 16-h anneal at  $975^\circ C$  in a  $N_2$  ambient in an  $Al_2O_3$  boat. The  $975^\circ C$  anneal produced

strong red Li-Li-O luminescence after subsequent Li diffusion, whether or not the crystals had been Li diffused prior to the anneal. Other O-doped LEC crystals grown from a Ga-rich melt (90% Ga) at reduced temperatures (grown at  $\sim 1200^\circ C$ , quenched from  $\sim 1100^\circ C$ ) showed the red Li-Li-O luminescence clearly after similar Li diffusions with no  $975^\circ C$  preanneal. Crystals grown<sup>9</sup> from Ga solution at  $\sim 1100^\circ C$  generally showed the red Li-Li-O luminescence on Li diffusion of the virgin crystals, especially those deliberately doped with O. Gallium phosphide needles and blades grown by wet hydrogen transport (the Frosch method<sup>10</sup>) invariably showed strong red Li-Li-O luminescence after standard Li diffusion, unlike crystals grown from the vapor by the halide transport process, which contain very low concentrations of O.

Two Li-diffusion techniques were employed. Most diffusions were done from Li vapor at  $700^\circ C$ . The crystals to be diffused were placed in a Ta tube together with a small pellet of unoxidized Li metal, adequate to produce the saturated vapor pressure. The Ta provides a suitable reducing atmosphere which minimizes the effect of any surface oxidation of the Li pellet. The ends of the tube were pinched off, and the tube was then sealed off in a small fused  $SiO_2$  ampoule. The Ta tube was also necessary to prevent an explosive reaction between Li and the fused  $SiO_2$  ampoule otherwise possible at the diffusion temperature.<sup>11</sup> As far as possible all manipulations were performed in a glove box under an Ar atmosphere and the Ta tube and fused  $SiO_2$  ampoule were carefully cleaned with  $HNO_3$  containing a small amount of HF to minimize oxidation of the Li metal. The fused  $SiO_2$  ampoule was fire polished and sealed off under a vacuum of  $10^{-4}$  mm Hg. The ampoule was heated to the desired diffusion temperature (usually  $700^\circ C$ ) in a muffle furnace, arranged so that rapid quenching in a water bath at the end of the desired diffusion time (usually  $\sim 60$  min) was possible. The GaP crystals darkened noticeably under this treatment. Large surface regions usually became roughened where contacted by excess Li metal, which was dissolved in an  $H_2O$  bath immediately after the crystals were removed from the fused  $SiO_2$  ampoules. The crystals usually showed uniform red Li-Li-O luminescence after the standard diffusion ( $700^\circ C$ , 60 min), from beneath the unattacked (smooth) surface regions and from the roughened regions alike, especially for the vapor-grown crystals. At diffusion temperatures  $\leq 500^\circ C$  the red luminescence was patchy even from the vapor-grown crystals. Diffusion at  $\geq 800^\circ C$  in vapor-grown GaP resulted in severe attack and disintegration of the crystals.

The second diffusion method followed the technique of Pell.<sup>12</sup> The crystal surfaces were coated with a suspension of Li in mineral oil. They were

then heated in a  $N_2$  atmosphere to  $\sim 700^\circ C$  on a strip heater, when a red surface glow was observed, possibly indicative of an exothermic surface alloying reaction. Finally, the crystals were placed in a Mb boat with a close-fitting lid, flushed out with  $N_2$ , and annealed at  $700^\circ C$  for 12 h in a muffle furnace. These times were far from minimal for the diffusion, but had been found ample to ensure success in the uniform compensation of large slices of crystal up to 1 cm thick required for infrared absorption studies.<sup>13</sup> As in the first method, visual indication of the vigorous Li- $H_2O$  reaction when the crystals were rinsed was usually good evidence of a successful diffusion. Infrared studies indicated that this treatment provided uniform compensation to a carrier concentration  $\lesssim 10^{14} \text{ cm}^{-3}$  in  $p$ -type material with initial concentrations as high as  $10^{18} \text{ cm}^{-3}$  or more. Compensation also occurred for  $Ga_2O_3$ -doped LEC crystals which were weakly  $n$  type (in the low  $10^{16}\text{-cm}^{-3}$  range) probably due to O donors, but not in more strongly  $n$ -type material deliberately doped with shallow donors such as S. The notion that the O donors are compensated by Li diffusion is also supported by the observation of strong quenching of the intensity of infrared electron-capture luminescence.<sup>14</sup> In this respect Li diffusion into GaP seems to produce compensation properties similar to those found in Si<sup>15</sup> but not in GaAs where compensation of both  $n$ - and  $p$ -type material is possible.<sup>16</sup>

### B. Optical Measurements

The luminescence spectra were usually recorded photographically with a Bausch and Lomb  $f/17$  spectrograph. The crystals were freely suspended in liquid He,  $H_2$ , or  $N_2$  and excited by a 4880-Å light from an  $Ar^+$  laser. Lifetime measurements were made using an acousto-optical modulator for the  $Ar^+$  laser as described elsewhere.<sup>17</sup> Optical absorption spectra and the temperature quenching of the red Li-Li-O luminescence were obtained using a Spex 1401  $f/6.8$  scanning double monochromator. In these measurements, the crystals were cooled in a stream of cold He gas to controlled temperatures in the range 15 to  $\sim 200^\circ K$ .

## III. RESULTS AND DISCUSSION

### A. Red Li Luminescence Spectrum

Gallium phosphide crystals grown from Ga solution (particularly when O doped) and from vapor by wet  $H_2$  transport invariably show a bright red low-temperature luminescence when Li diffused under standard conditions ( $700^\circ C$ , 60 min—see Sec. II A). The spectrum of this efficient luminescence contains considerable structural detail. A single strong sharp line  $Li_{L_2}^0$  at 2.0874 eV dominates the  $1.6^\circ K$  spectrum [Fig. 1(a)], with a broad structured wing to lower energy. The sharp struc-

ture superposed on the high-energy portion of the wing shown in Fig. 1(a) can be accounted for in terms of phonon replicas of the line  $Li_{L_2}^0$ . For example, the replica involving the 50.1-meV  $LO(\Gamma)$  phonon is clearly seen and forms a high (phonon) energy limit to the group of closely spaced optical phonon replicas, as expected from the energy spectrum of phonons in GaP.<sup>18</sup> The  $LO(\Gamma)$  replica of the weak line  $Li_{L_1}^0$ , 0.99 meV below  $Li_{L_2}^0$ , is also prominent. This behavior is very reminiscent of the spectrum of excitons bound to N isoelectronic traps in GaP.<sup>1</sup> Additional similarities between the N and red Li luminescence spectra include the presence of broad phonon replicas, such as  $Li_{L_2}^{LA}$  and  $Li_{L_2}^{LA}$  in Fig. 1(a). These replicas are the form of the density of states of the TA and LA branches of the GaP normal modes, although their relative intensities are different. Also, the replica  $Li_{L_2}^T$  in Fig. 1(a) may involve the  $TO(\Gamma)$  phonon characteristic of the GaP lattice, which is prominent in the N spectrum,<sup>1</sup> although the energy is slightly high (Table I).

Thermalization occurs between lines  $Li_{L_1}^0$  and  $Li_{L_2}^0$ , and  $Li_{L_1}^0$  is not seen at  $20.6^\circ K$  [Fig. 1(b)]. However, line  $Li_{L_1}^0$  is always weak even at the lowest temperatures in strain-free crystals<sup>19</sup> and evidently represents a forbidden transition. Differences in the general form of the phonon sideband between 1.6 and  $20.6^\circ K$  (Fig. 1) are probably mainly due to the thermal quenching with  $Li_{L_1}^0$  of phonon replicas of this line. Evidently the predominant decay mode from the lowest-energy initial state involves phonon-assisted transitions. Thus far, the spectrum is again very reminiscent of N in GaP.<sup>1</sup> However, Fig. 1(b) also shows two additional no-phonon lines  $Li_{L_{3,4}}^0$  about 3 meV above  $Li_{L_2}^0$ , unlike the N luminescence spectrum which contains just two thermalizing no-phonon lines. These additional lines bear a constant ratio to  $Li_{L_2}^0$ , independent of excitation intensity, at a given temperature. The shoulder  $Li_{L_4}^0$  is clearly seen as a separate component in the original photographic data, but smears into  $Li_{L_3}^0$  in the densitometer readout since lines  $Li_{L_{3,4}}^0$  are broad. Presumably the broadening is a lifetime effect, like that studied for a red luminescence center in ZnTe (the O isoelectronic trap) which has two widely spaced no-phonon lines which thermalize in luminescence.<sup>20</sup> Lines  $Li_{L_{2,3,4}}^0$  can be seen in absorption (Sec. III E), where no thermalization occurs. Thus, the red Li luminescence spectrum contains four no-phonon lines, due to small splittings of the initial state of the luminescence transition. There is no experimental evidence for a splitting in the final state. A  $j$ - $j$  coupling model accounting for this property is presented in Sec. III B.

The red Li luminescence spectrum also differs sharply from the N spectrum in the presence of a

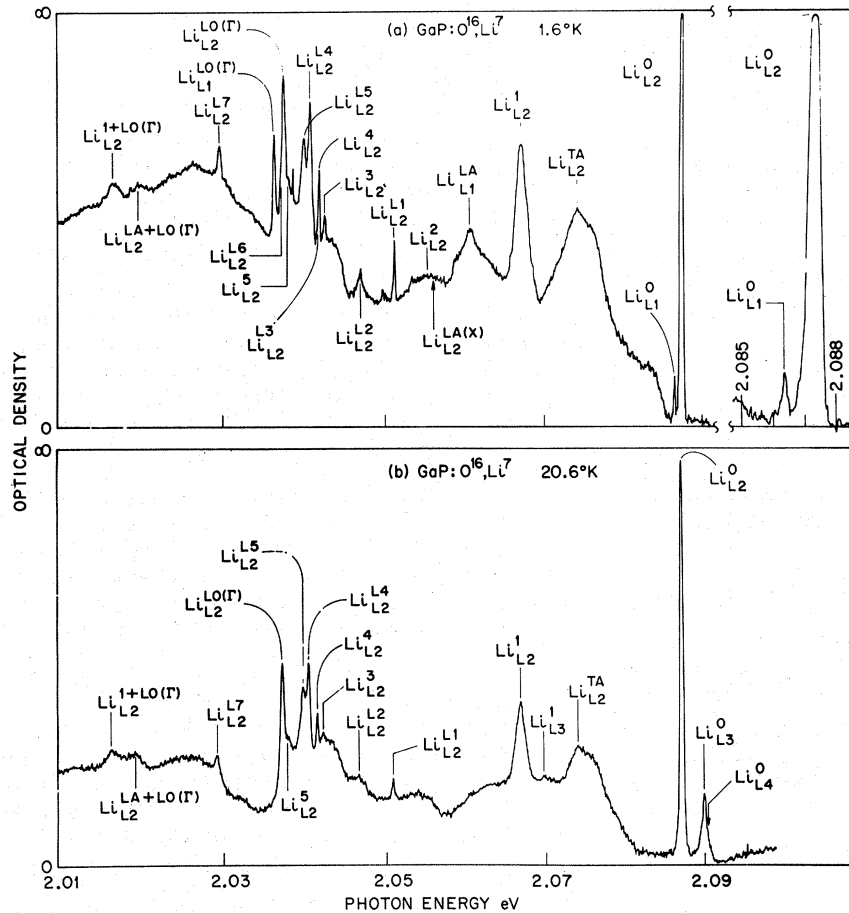


FIG. 1. Portions of the low-temperature photoluminescence spectra from O-doped Li-diffused GaP showing the detailed structure of the Li-Li-O bound exciton transitions, recorded photographically. Superscripts denote whether the component is due to no-phonon (0) or phonon-assisted electronic transitions. The type of phonon is indicated, either specifically [e.g., LO( $\Gamma$ ), TA, etc.], or with arbitrary notation which differentiates between phonons whose energy is significantly dependent on the mass of the Li or O atom (components LN) and others (components N) which are not anticipated from the normal-mode vibrational spectrum of the GaP lattice. These spectra are characteristic of GaP doped with the natural isotopes O<sup>16</sup> and (essentially) Li<sup>7</sup>. Spectrum (a) is recorded at 1.6°K. The two no-phonon lines visible at this temperature are shown in greater detail in the right-hand portion. Additional no-phonon lines become visible at 20°K [spectrum (b)].

large number of lines on the phonon wing *beyond* those anticipated from the normal-mode vibrational spectrum of the GaP lattice. These cannot be additional electronic transitions at the same center,

TABLE I. Phonons resolved in the sideband of the red Li luminescence.<sup>a</sup>

	Local modes		GaP normal modes	
	Phonon	Energy (meV) L <sup>b</sup> A <sup>c</sup>	Phonon	Energy (meV) L <sup>b</sup> A <sup>c</sup>
Local	L6	50.3		
	L7	57.9	TA(L)	11.1
Gap	L1	36.3, 33.2	TA(X)	13.2, ~13
	L2	40.5 36.0		
In-band resonance	1	20.4, 20.4	LA(L)	25.7
	2(?)	32.2	4[TO( $\Gamma$ )?]	45.6
	3	44.9		
	5	49.4	LO( $\Gamma$ )	50.0
	L3	45.8		
	L4	46.7	LA(L) + LO( $\Gamma$ )	67.7
	L5	47.5 47.5		

<sup>a</sup> Measured for the "standard" isotope combination Li<sup>7</sup>, O<sup>16</sup> [Fig. 1(a)].

<sup>b</sup> Measured in luminescence.

<sup>c</sup> Measured in absorption and luminescence excitation.

since no thermalization into them occurs from Li<sub>L2</sub><sup>0</sup>. They exhibit a constant intensity relative to Li<sub>L1,2</sub><sup>0</sup> in strain-free crystals, even for different types of crystal Li diffused under different conditions. This implies that they are not due to electronic transitions at independent centers comprising higher associates of the center responsible for Li<sub>L2</sub><sup>0</sup> [unlike, for example, the nearest-neighbor (NN) lines in GaP<sup>1</sup>]. The only other obvious possibility is that they are due to the electronic transitions responsible for Li<sub>L1,2</sub><sup>0</sup> in which "local-mode" phonons are emitted. These phonons are "local" in the sense that they involve perturbations in the density of states of the GaP lattice normal-mode spectrum induced by the presence of the defect responsible for the Li<sub>L1,2</sub><sup>0</sup> lines. In the language of impurity-induced lattice vibrations,<sup>21</sup> some of these extra phonons involve true "local modes," with energies above the cutoff of the GaP vibrational spectrum [for example, Li<sub>L2</sub><sup>L6</sup>, Li<sub>L2</sub><sup>L7</sup> in Fig. 1(a) and Table I]. Others are "gap modes," occurring in the gap between the acoustical and optical branches of the GaP normal modes<sup>22</sup> [Li<sub>L2</sub><sup>L1</sup> and Li<sub>L2</sub><sup>L2</sup> in Fig. 1(a) and Table I]. Still others are "in-band resonance modes," impurity-induced enhancements of

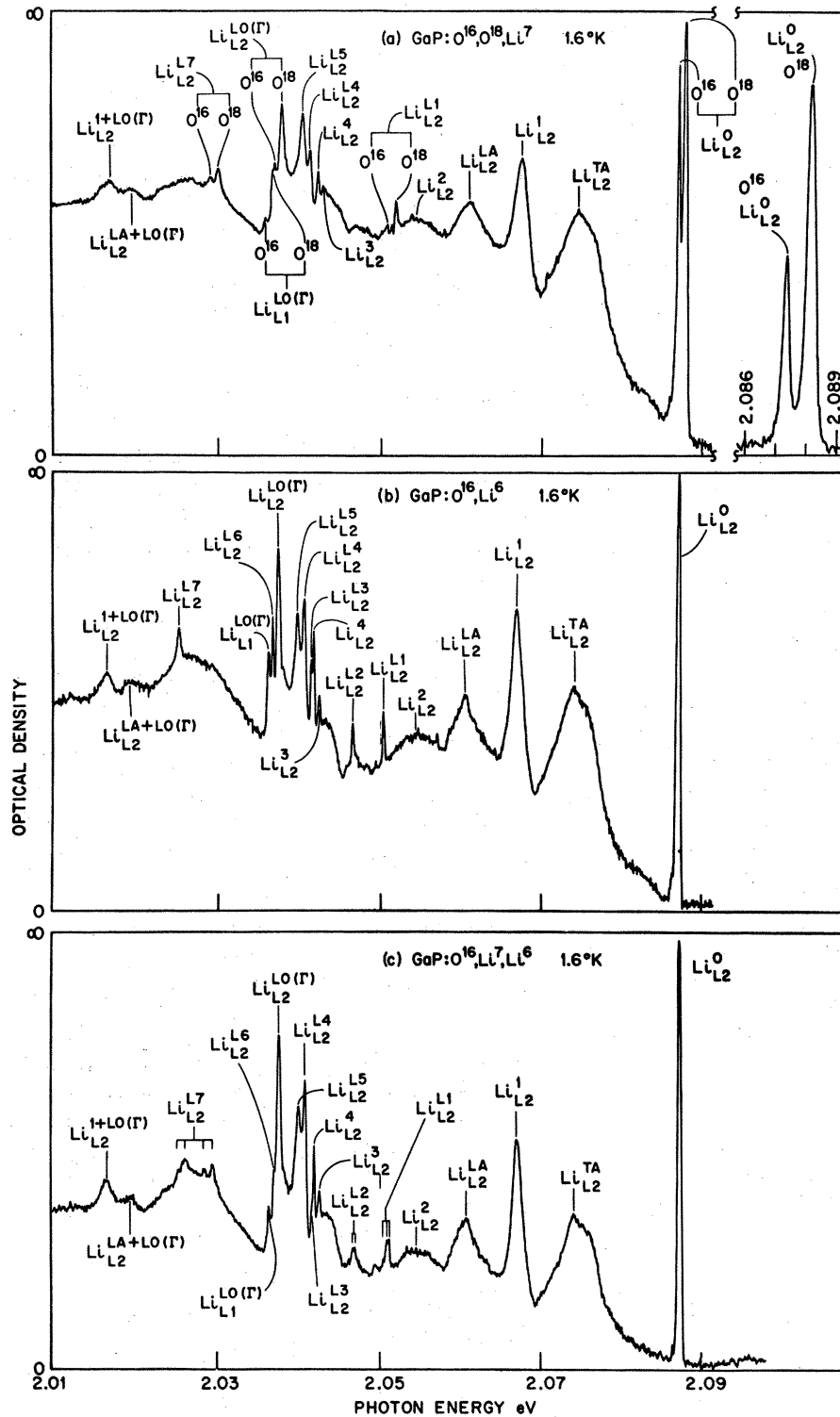


FIG. 2. Portions of the low-temperature photoluminescence spectra from Li-diffused GaP, recorded photographically. The notation is identical with Fig. 1. Part (a) was obtained from a crystal doped with  $O^{18}$  and diffused with  $Li^7$ . Some  $O^{16}$  was also present, indicating inadvertent contamination during crystal growth. The right-hand portion shows details of the isotope shift of the principal  $Li_{L_2}^0$  no-phonon line observed for the substitution  $O^{16} \rightarrow O^{18}$ . Some of the phonon energies determined from the vibronic structure are also changed by this substitution (Table II). Part (b) was obtained from an  $O^{16}$ -doped  $Li^6$ -diffused crystal. The substitution  $Li^7 \rightarrow Li^6$  produces no detectable shift in the no-phonon energies, but many of the phonon energies in the vibronic structure are appreciably increased (Table II). Part (c) was obtained from an  $O^{16}$ -doped crystal diffused with Li from a source containing nearly equal proportions of  $Li^6$  and  $Li^7$ . Attention is directed to the vibronic structure labelled  $Li_{L_2}^{L_7}$ , where four peaks are resolved rather than just the two anticipated for a complex containing only one Li atom. Note that the detailed form of the coupling to the optical phonon replicas near 2.04 eV is particularly sensitive to the mass of the O isotope [compare (a) and (b), also (b) with Fig. 1(a)].

narrow portions of the GaP normal-mode frequency spectrum which normally contain a low density of states [ $Li_{L_2}^1$ ,  $Li_{L_2}^3$ ,  $Li_{L_2}^4(?)$ ,  $Li_{L_2}^5$ ,  $Li_{L_2}^6$ , and possibly others].

The assignment of these lines as local modes is

proved for many by the isotope shifts determined from Fig. 2 and listed in Table II. The energies of the replicas with superscript  $LN$  are generally relatively sensitive to the mass of the Li atom diffused into the crystal, but are appreciably less sensitive to

TABLE II. Isotope shifts in "local modes" of the Li-Li-O complex.

Mode	Type	Isotope shift (meV)		$f_{KE}$	
		$\hbar\omega(\text{Li}^6) - \hbar\omega(\text{Li}^7)$	$\hbar\omega(\text{O}^{18}) - \hbar\omega(\text{O}^{16})$	Li	O
L6	Local	+0.45	?	0.12	?
L7		+4.23	-0.29	1.02	0.08
L1	Gap	+0.75	-0.33	0.29	0.15
L2		+0.45	?	0.16	?
1	In-band resonance	+0.05	-0.04 (?)	0.03	0.03
3		+0.05	-0.08	0.02	0.03
4(?)		+0.06	-0.07	0.02	0.025
L3		+0.10	?	?	?
L4		+0.08	-0.19	0.02	0.065
L5		+0.18	-0.10	0.05	0.035

the mass of the heavier O atom. This is expected, even though the percentage changes in the Li and O masses are roughly comparable, since the relatively heavy O atom will possess a small proportion of the total kinetic energy of the local motion (Sec. III D). The percentage changes in energy induced by the isotopic substitutions are large for the true local modes, moderate for the gap modes, and very small for the in-band resonance modes, as anticipated from local-mode theory.<sup>21</sup> Additional discussion of these local modes will be reserved for Sec. III D. Here, we note only the appearance of *two* local-mode replicas on diffusion with a Li source containing approximately equal amounts of the isotopes Li<sup>6</sup> and Li<sup>7</sup> [Fig. 2(c)] in addition to the Li<sub>L2</sub><sup>7</sup> replicas seen in crystals diffused with pure Li<sup>6</sup> [Fig. 2(b)] and natural Li [92.6% Li<sup>7</sup>, Fig. 1(a)]. This proves that the center responsible for the red Li luminescence must contain *at least two inequivalent* Li atoms.

The existence of these isotope-induced shifts in the Li<sub>L1,2</sub><sup>0</sup> replicas provides unequivocal proof that both Li and O occur in the impurity center responsible for the red Li luminescence. Since this spectrum has never been seen other than in crystals deliberately diffused with Li, the incrimination of O is the more significant result. The most striking effect of the substitution O<sup>16</sup> - O<sup>18</sup> is the large (0.80-meV) shift to higher energies in the no-phonon lines, clearly shown for Li in Fig. 2(a). Qualitatively similar effects have been observed in the optical spectra of isolated O donors<sup>15,23</sup> and of nearest-neighbor Cd-O pairs<sup>3,4</sup> in GaP. This similarity is strong evidence that O is on P lattice sites in the red Li luminescence center, as for the other spectra. However, the detailed structure in the phonon wing is quite unlike that observed in the O-related spectra seen previously. Evidently the presence of Li plays a key role here (Sec. III D).

#### B. Li, O Model for Red Li Luminescence Center

We have shown in Sec. III A that the red Li lumi-

nescence spectrum contains four no-phonon lines, with thermalization between them, and a phonon sideband containing a wealth of structure. This spectral form suggests that the luminescence is due to the recombination of excitons bound to some defect by  $E_{bx} = (E_{gx} - \hbar\nu_{Li^0})$ ,  $\sim 0.24$  eV, where  $\hbar\nu_{Li^0}$  is an average no-phonon energy. Unequivocal proof that this center contains O and at least two inequivalent Li atoms was obtained. The simplest impurity center possessing these properties results from the substitution of P by O and an adjacent Ga by *two* Li atoms. The resulting center, written Li<sub>L</sub>-Li<sub>Ga</sub>-O<sub>P</sub> rather than Li<sub>2</sub>-O to emphasize the inequivalence of the Li atoms established from the local-mode studies, is isoelectronic with the Ga-P atom pair it replaces, since Li<sub>Ga</sub> is a double acceptor and Li<sub>L</sub> and O<sub>P</sub> are singly charged donors.

The isoelectronic character of this model is crucial in two ways. First, the high luminescence efficiency<sup>24</sup> and moderately long luminescence decay time (Sec. III E) observed at low temperatures show that the excited electronic state contains no electronic particles other than the exciton. If this were not so, nonradiative (Auger) recombinations would be overwhelmingly predominant, as can be seen from the extrapolation to large  $E_{bx}$  of the behavior found for shallow donor<sup>25</sup> and acceptor<sup>17</sup> exciton complexes in the indirect gap semiconductor GaP.

The assumption of a bare (isoelectronic) final state is also consistent with the presence of but a single zero-field ground-state energy level (Sec. III A) which is nondegenerate according to its behavior in a magnetic field (Sec. III C). Second, the Li-Li-O model provides an immediate semiquantitative understanding of the binding energy of the exciton. Oxygen is a donor of binding energy  $\sim 0.89$  eV on the P site in GaP.<sup>14,23</sup> The substitution of the two Li atoms for one of the four neighboring Ga atoms is equivalent to placing a single ionized acceptor on the adjacent lattice site. If this acceptor is regarded as a screened negative charge at the

normal Ga-P bond length from the O donor core, the electron binding energy  $E_e$  is reduced to  $\sim 0.4$  eV. This crude calculation works surprisingly well for the Zn-O and Cd-O isoelectronic pair substituents in GaP.<sup>23</sup> In the present example, the small size of the Li atom (as well as O) strongly suggests that the effective separation between O and its neighboring ionized acceptor will be significantly *less* than the normal Ga-P bond length. Using the sum of the covalent radii of Li and O,  $r_{\text{Li-O}} = 2.07 \text{ \AA}$ , the reduction factor  $e^2/\epsilon r_{\text{Li-O}}$  is  $\sim 0.65$  eV for  $\epsilon = 10.75$ . Thus, the predicted transition energy of the Li-Li-O exciton is  $E_g(2.34 \text{ eV}) - E_e[\sim(0.89 - 0.65) \text{ eV}] - E_h(\sim 0.03 \text{ eV}) \sim 2.07 \text{ eV}$ , in remarkably good agreement with the experimental value of  $\sim 2.09 \text{ eV}$  (Fig. 1). In this calculation,  $E_g$  is the energy gap of GaP and  $E_h$  is the binding energy of the hole to the electron at the Li-Li-O center. The assumption that the binding of the exciton is mainly due to the electron is also consistent with the Zeeman data discussed in Sec. III C and with the transition oscillator strength (Sec. III E).

Figure 3 contains a  $j$ - $j$  coupling scheme for an exciton bound to a  $\langle 111 \rangle$  uniaxial center of  $C_{3v}$  symmetry, such as is the most elementary model for the Li-Li-O complex (like Cd-O<sup>4,26</sup>). In a cubic crystal field, the  $s = \frac{1}{2}$  electron, bound to an electron-attractive P-site substituent,<sup>27</sup> combines with the  $j = \frac{3}{2}$  hole to form  $J = 1$  and  $J = 2$  states. The

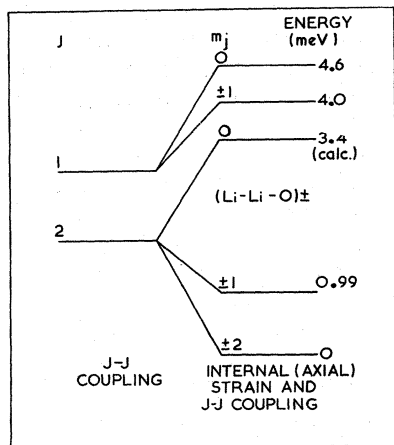


FIG. 3. Electronic states formed by binding an exciton to an electron-attractive center with  $C_{3v}$  symmetry in GaP, drawn approximately to scale as appropriate for the Li-Li-O associate. Two states separated by  $\Delta$  are formed by  $J$ - $J$  coupling between a  $j = \frac{3}{2}$  hole and a spin- $\frac{1}{2}$  electron (left). These states split in the axial field of the  $C_{3v}$  center as shown to the right, where  $m_j$  is defined relative to the axial crystal field. The  $|2, 0\rangle$  and  $|2, \pm 2\rangle$  states have separated by  $2\epsilon_0$  in the axial field, like the  $\Gamma_8$  hole state. More precise experimental values for the energies shown on the right are 0.99, 3.86, and 4.54 meV.

$J = 2$  state lies lowest because the hole and electron have opposite charge. Electric dipole transitions are allowed only from the  $J = 1$  state. The  $J = 2$  state may be split in the cubic crystal field, as observed for the isoelectronic trap Bi in GaP,<sup>28</sup> but no mixing of the  $J = 1$  and  $J = 2$  states occurs. Under  $\langle 111 \rangle$  uniaxial crystal field, such as is characteristic of a  $C_{3v}$  symmetry center, the  $J = 1$  and  $J = 2$  states both split as shown.<sup>4,29</sup> The total angular momentum  $J$  is no longer a good quantum number, but the  $z$  component of the angular momentum  $m_j$  remains a constant of the motion, where  $z$  is defined along the  $\langle 111 \rangle$  symmetry axis of the center. The energies given in Fig. 3 are experimental. The four relative separations are defined in terms of two parameters, a  $J$ - $J$  coupling (exchange) energy  $\Delta$  and a parameter  $\epsilon_0$ , where  $2\epsilon_0$  is the splitting of the  $\Gamma_8$  hole state under the uniaxial crystal field. The energy of the  $m_j = \pm \frac{3}{2}$  hole state is *lowered* by  $2\epsilon_0$  compared with the  $m_j = \pm \frac{1}{2}$  state under the uniaxial tension produced on replacing Ga-P by the small complex Li-Li-O. This situation has been analyzed by Morgan and Morgan.<sup>29</sup> They were specifically interested in the Cd-O pair in GaP, where only the lower two states shown in Fig. 3 were clearly defined by experiment. However, Morgan and Morgan give general expressions for the energies of the complete set of five components for arbitrary  $\Delta$ ,  $\epsilon_0$ . The set of experimental energies in Fig. 3 is approximately consistent with their Table I if  $\Delta = 1.1$  meV and  $\epsilon_0 = 1.7$  meV. An alternative solution,  $\Delta = 3.4$ ,  $\epsilon_0 = 0.56$  meV, is discarded because of evidence from the relative line intensities (below).

The two  $m_j = \pm 1$  states become mixed by the uniaxial field, unlike the  $m_j = 0$  or  $\pm 2$  states. This follows since the  $m_j = \pm 1$  component from  $\Gamma_5$  ( $J = 1$ ) state has a wave function which transforms like  $(x \pm iy)$  which can be written as  $\pm iz(x \mp iy)$  for the  $T_d$  group. Thus this state mixes with the  $\pm 1$  component from the  $J = 2$  state, which transforms like  $z(x \pm iy)$ . Clearly, the  $m_j = +1$  state from  $J = 1$  couples with the  $m_j = -1$  state from  $J = 2$ , and vice versa. The  $m_j = 0$  state from  $J = 1$  transforms like  $z$ , i. e.,  $xy$ , and has zero matrix element with the  $m_j = 0$  state from  $J = 2$ , which transforms like  $z^2$ . The  $m_j = \pm 2$  state from  $J = 2$  transforms like  $(x \pm iy)^2$ , and does not interact with any component from the  $\Gamma_5$  state because  $m_j$  is a good quantum number for  $C_{3v}$  symmetry.

Three allowed transitions are predicted on this model, and are identified with lines  $\text{Li-Li-O}_{2,3,4}^0$  from Fig. 1. There are two forbidden transitions, ordered as shown in Fig. 3. The  $m_j = \pm 2$  state lies lowest and can be preferentially populated at sufficiently low temperatures. The  $J = 2$ ,  $m_j = 0$  state is not seen experimentally.

In the weak crystal-field limit, there are just

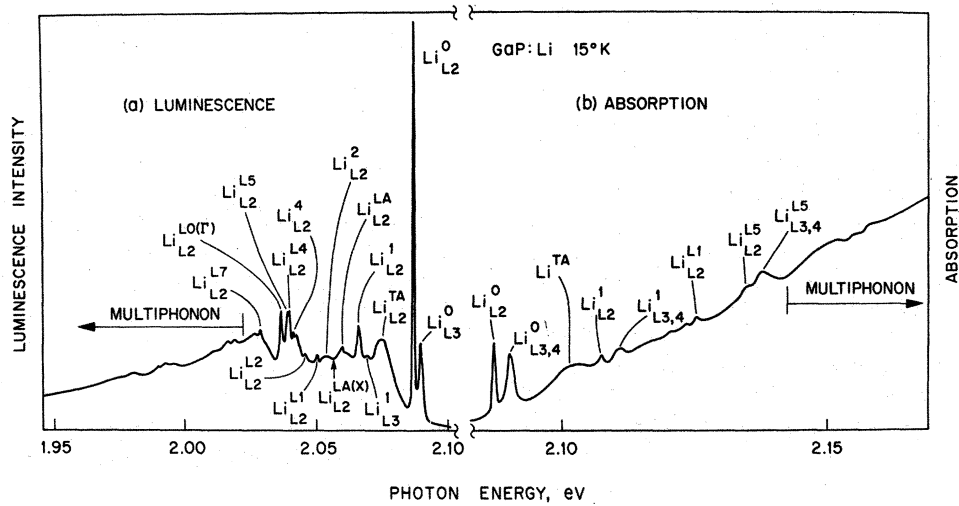


FIG. 4. (a) A portion of the low-temperature photoluminescence of an O-doped Li-diffused GaP crystal, recorded photoelectrically. (b) A portion of the low-temperature optical transmission spectrum of a similar crystal, also recorded photoelectrically. The absorption coefficient near the peaks  $\text{Li}_{L_2}^0$ ,  $\text{Li}_{L_{3,4}}^0$  is  $\sim 0.5 \text{ cm}^{-1}$ . The general decrease in the signal level to the right is partly due to changes in the light intensity incident on the sample from the W source. Note that the energy scale in (b) is magnified 2 times compared with (a).

two allowed transitions, from the  $m_j = 0, \pm 1$  states of  $J=1$ . The intensity ratio  $I_{\pm 1}/I_0 = 2$ . For complete mixing, under a sufficiently large axial field, the intensity ratio  $I_{\pm 1}^2/I_{\pm 1}^1 = 3$ . The relative intensities of the three allowed transitions from the  $|1, 0\rangle$ ,  $|1, \pm 1\rangle$ , and  $|2, \pm 1\rangle$  initial states will then follow the ratios  $1 : \frac{1}{2} : \frac{3}{2}$ , respectively. This condition is close to that exhibited by the absorption spectrum in Fig. 4(b), with regard to the ratio  $I_{0, \pm 1}^1/I_{\pm 1}^2$ . The dependence of the oscillator strength ratio  $R$  of the absorption transitions to the  $|2, \pm 1\rangle$  and  $|1, \pm 1\rangle$  states on  $\epsilon_0$ ,  $\Delta$  is predicted by the theory of Morgan and Morgan,<sup>29</sup> and is given by

$$R = \frac{1}{3} \{ [(\Delta/\epsilon_0 - 1)^2 + 3]^{1/2} - (\Delta/\epsilon_0 - 1) \}^2. \quad (1)$$

Equation (1) predicts that  $R \sim 1.5$  for  $\Delta = 1.1$ ,  $\epsilon_0 = 1.7 \text{ meV}$ ;  $R \sim 0.1$  for the complementary solution  $\Delta = 3.4$ ,  $\epsilon_0 = 0.56 \text{ meV}$  mentioned above. The intensity ratio of the relevant no-phonon lines in Fig. 4(b) is much closer to the result for the former parameter set, although the experimental  $R$  is slightly larger than predicted. This fact, together with the small difference between the experimental energy intervals  $h\nu_{|1,0\rangle} - h\nu_{|1,\pm 1\rangle}$  and  $h\nu_{|2,\pm 1\rangle} - h\nu_{|2,\pm 2\rangle}$  in Fig. 3, which are predicted to be equal on the model of Morgan and Morgan,<sup>29</sup> suggests that the Li-Li-O center may be more complicated in some sense than assumed in the model. The origin of this complication remains undetermined. However, it is likely that an appreciable part of the residual discrepancy for the intensity ratio  $R$  arises from differences in the phonon cooperation of the  $\text{Li}_{L_2}^0$  and  $\text{Li}_{L_3}^0$  lines, since the total absorption should be compared with the theoretical  $R$  from Eq. (1).

Unfortunately, it is impossible to obtain a quantitative estimate of this effect, although Fig. 4(b) suggests qualitatively that the phonon coupling is stronger for transitions to the  $|1, \pm 1\rangle$  state, as required, at least for some well-resolved sidebands. In view of this problem, and the fact that the  $h\nu_{|1,0\rangle} - h\nu_{|1,\pm 1\rangle}$  energy separation is hard to measure accurately, the deviations of the Li-Li-O exciton from the predictions of the simple model of Morgan and Morgan should not be taken too seriously. There is no doubt that the Li-Li-O cen-

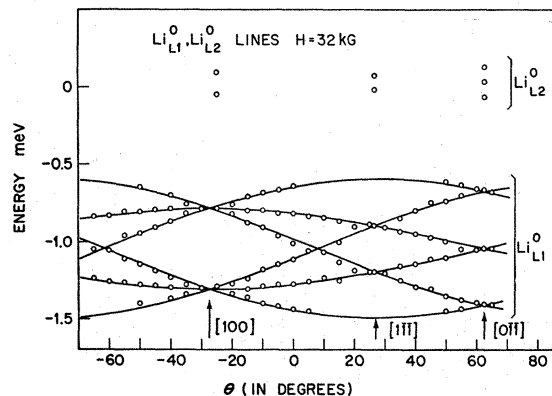


FIG. 5. Variation of the energies of the magnetic sub-components from no-phonon lines  $\text{Li}_{L_2}^0$  and, particularly,  $\text{Li}_{L_1}^0$  as the magnetic field is rotated in a  $\langle 110 \rangle$  plane. Specific principal crystal axes are indicated. The points are experimental for  $H = 32 \text{ kG}$ , the full lines, theoretical for transitions from a  $J=2$ ,  $m_j = \pm 2$  state to a  $J=0$  state for centers with  $\langle 111 \rangle$  symmetry axes (four equivalent orientations for  $H=0$ ), using the  $g$  values in Eq. (3).



ter has  $\langle 111 \rangle$ -type axial symmetry (Sec. III C).

### C. Zeeman Effect of Red Li Luminescence

The observation that the mixing of the two  $m_j = \pm 1$  states of the Li-Li-O center approaches the infinite crystal-field limit has important consequences for the interpretation of the Zeeman spectra. Figure 5 shows the energy anisotropy of the magnetic subcomponents representing transitions from the  $J=2m_j = \pm 2$  and  $\pm 1$  states as the crystal is rotated about the magnetic field in a  $\langle 110 \rangle$  plane. The strongly anisotropic behavior is very reminiscent of that observed for excitons bound to the Cd-O center in GaP.<sup>4,28</sup> The data are well fitted by the theoretical curves, calculated assuming that the uniaxial field has  $\langle 111 \rangle$  symmetry and that the ground state is nonparamagnetic. Each excited state is assumed to split into just two magnetic substates, separated by an energy  $\Delta E_H$  given by

$$\Delta E_H = g_{\text{eff}} \mu_B H \cos \theta. \quad (2)$$

Here  $\theta$  is the angle between  $H$  and the  $\langle 111 \rangle$  crystal field, i. e., the symmetry axis of the  $C_{3v}$  center, and  $\mu_B$  is the Bohr magneton. The  $g$  factor  $g_{\text{eff}}$  was obtained by fitting to experiment for

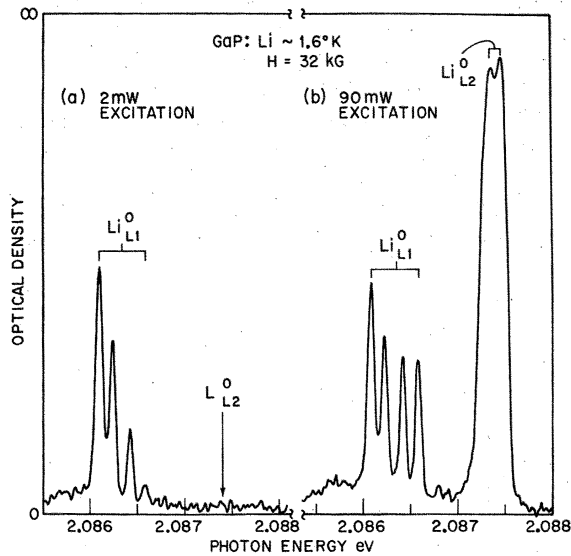


FIG. 6. Portions of the low-temperature photoluminescence of the Li-Li-O bound exciton in GaP, recorded photographically, showing the magnetic subcomponents of no-phonon lines  $\text{Li}_{L1}^0$  and  $\text{Li}_{L2}^0$  for  $H=32$  kG. Two sets of subcomponents are resolved for this orientation of the magnetic field (near  $\theta = -5^\circ$  in Fig. 5). At low intensity of optical excitation, in part (a), the populations of the exciton states are consistent with the Boltzmann factor for the temperature of the He bath. Thus transition  $\text{Li}_{L2}^0$  is not seen and the higher-energy magnetic subcomponents from  $\text{Li}_{L1}^0$  are weak. In part (b) the system is not at equilibrium with the He bath under high-intensity optical pumping, and the relative intensities of the higher-energy components rise dramatically.

TABLE III.  $g$  values for a  $C_{3v}$  center in GaP.

State ( $J, m_j$ )	$g$ value <sup>a</sup>	
	Low crystal field	High crystal field
1, $\pm 1$	$\frac{1}{4}(5g_h - g_e)$	$\frac{1}{2}(g_e + g_h)$
2, $\pm 1$	$\frac{1}{4}(3g_h + g_e)$	$\frac{1}{2}(3g_h - g_e)$
2, $\pm 2$	$\frac{1}{2}(3g_h + g_e)$	$\frac{1}{2}(3g_h + g_e)$

<sup>a</sup>These factors are defined directly by the expression  $\Delta E = g\mu_B H$  for the Zeeman splitting  $\Delta E$ . The hole anisotropy parameter  $L$  is assumed to be zero, and only the linear Zeeman effect is considered.

$H \parallel \langle 100 \rangle$ , where only two components are observed for each of  $\text{Li}_{L1}^0$  and  $\text{Li}_{L2}^0$  since all four possible  $\langle 111 \rangle$  axes are equally inclined to the magnetic field. Figure 5 shows that the fit between theory and experiment is excellent for the  $\text{Li}_{L1}^0$  line, where  $g_{\text{eff}}$  is substantial. Meaningful data could only be obtained for  $H$  parallel to high-symmetry axes for  $\text{Li}_{L2}^0$ , since  $(g_{\text{eff}})_{\text{Li}_{L2}^0} \sim \frac{1}{4}(g_{\text{eff}})_{\text{Li}_{L1}^0}$  and the line  $\text{Li}_{L2}^0$  is slightly broader than  $\text{Li}_{L1}^0$  in zero magnetic field.

All of the above assumptions are consistent with the model shown in Fig. 3. Thermalization shown in Fig. 6 between the magnetic subcomponents of the  $\text{Li}_{L1}^0$  line, as well as between zero-field lines  $\text{Li}_{L2}^0$  and  $\text{Li}_{L1}^0$ , supports the assertion that all the splittings occur in the initial state of the luminescence transition. The  $\langle 111 \rangle$  symmetry axis suggests that the Li atoms are aligned along a bond between the O atom and the Ga site. We have seen that a Ga vacancy must be present to obtain the correct (neutral) charge state of the center (Sec. III B). This aspect of the model will be discussed further in Sec. III D.

The high and low crystal-field limits for the  $g$  values of the three Kramers-doublet initial states of a  $C_{3v}$  center such as  $\text{Li}_i\text{-Li}_{\text{Ca}}^i\text{-O}_p$  in GaP, defined for  $H \parallel z$ , are given in Table III. Using the high-field limits, because of the evidence from the oscillator strength of the transition  $\text{Li}_{L2}^0$  from the  $J=2, m=\pm 1$  state mentioned above, we conclude from the fit to the data in Fig. 5 that

$$\left(\frac{3}{2}g_h + \frac{1}{2}g_e\right) = 2.44 \pm 0.1,$$

$$\left(\frac{3}{2}g_h - \frac{1}{2}g_e\right) = 0.68 \pm 0.1.$$

Thus

$$g_h = 1.04 \pm 0.05,$$

$$g_e = 1.76 \pm 0.14. \quad (3)$$

These values are consistent with those obtained<sup>14,28</sup> for the Cd-O complex in GaP and also agree with earlier data for the electron-attractive P-site donor S.<sup>27</sup>

Figure 7 shows that the splittings with magnetic field of the transitions  $\text{Li}_{L1}^0$  and  $\text{Li}_{L2}^0$  are slightly nonlinear. This is due to magnetic interactions be-

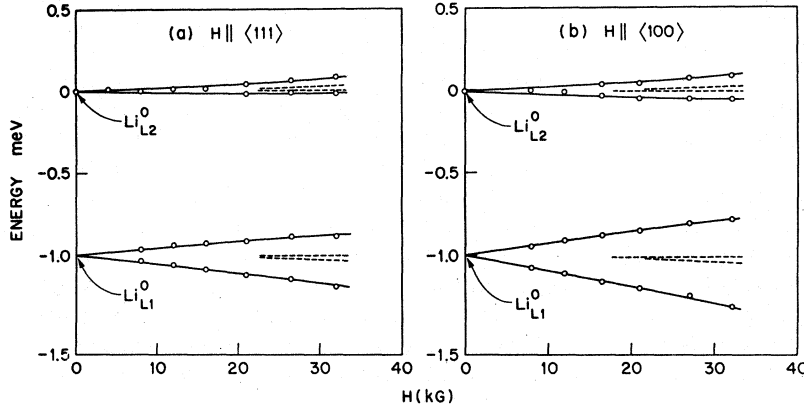


FIG. 7. The variation with  $H$  of the energies of magnetic subcomponents of the no-phonon lines  $Li_{L1}^0$  and  $Li_{L2}^0$  of the Li-Li-O exciton (a) for  $\vec{H} \parallel \langle 111 \rangle$  and (b) for  $\vec{H} \parallel \langle 100 \rangle$ . The points are experimental; the full lines are drawn according to the  $g$  values in Eq. (3) with a nonlinear component arbitrarily adjusted for best fit to the data points. The extent of the nonlinear shift is emphasized by the dashed lines, drawn to follow the center of gravity of the observed components and also for zero nonlinear shift. Only the intense magnetic subcomponents with small splittings, from the three equivalent sets of  $\langle 111 \rangle$  centers *not* parallel with  $H$ , are shown for  $\vec{H} \parallel \langle 111 \rangle$ . The set aligned with  $H$  shows much larger splitting (Fig. 5), but the probabilities of the relevant transitions are very low [Eq. (4)]. Only one pair of magnetic subcomponents is expected from each of  $Li_{L1}^0$  and  $Li_{L2}^0$  for  $\vec{H} \parallel \langle 100 \rangle$ .

tween the  $J=2$ ,  $m=\pm 1$  and  $J=2$ ,  $m=\pm 2$  excited states. We do not feel that the nonlinear behavior is defined sufficiently precisely by the present data to warrant a detailed analysis. Nevertheless, it is interesting to note that the magnitude of the nonlinear shifts at 32 kG in Fig. 7 are about twice the corresponding values for the N isoelectronic trap in GaP,<sup>30</sup> even though the interacting lines are slightly closer for  $N$  ( $\sim 0.87$  meV, cf. 0.99 meV for Li-Li-O). The nonlinear term is expected to be relatively small for a  $T_d$  symmetry center like  $N$ , since it is nonzero in this case only as a result of deviations of  $g_e$  and  $g_h$  from the free-electron value of 2.

The identification of the  $J=1$ ,  $m=0$  and  $m=\pm 1$  states, respectively, with components  $Li_{L3}^0$  and  $Li_{L4}^0$  of the Li-Li-O spectrum is strengthened by Zeeman data taken at 20.6°K. The breadth of line  $Li_{L3}^0$  is about four times that of line  $Li_{L2}^0$ , and the magnetic subcomponents of  $Li_{L3}^0$  were not resolved. However, the additional broadening of  $Li_{L3}^0$  at  $H=32$  kG  $\parallel \langle 100 \rangle$  was consistent with a  $g_{eff}$  of order 2 times that of  $Li_{L2}^0$ , in agreement with the ratio  $2.06 \pm 0.35$  predicted from Table III using the  $g$  values in Eqs. (3).

The mixing of the  $J=2$ ,  $m_j=\pm 1$  and  $J=2$ ,  $m_j=\pm 2$  states due to the magnetic field is expected to give the following ratio of transition rates  $W$  for lines  $Li_{L1}^0$  and  $Li_{L2}^0$ :

$$\frac{W_{L1}}{W_{L2}} = \left( \frac{g_e \mu_B H \sin \theta}{\hbar \nu_{L2} - \hbar \nu_{L1}} \right)^2. \quad (4)$$

Qualitative evidence of the  $\sin^2 \theta$  proportionality was obtained from the fact that the magnetic sub-

components of  $Li_{L1}^0$  became unobservably weak in a strain-free crystal near their maximum Zeeman splitting (Fig. 5). The dependence on  $H^2$  is quantitatively substantiated by the data in Fig. 8.

#### D. Analysis of Li-Li-O "Local Modes"

No detailed analysis of the local-mode energies will be offered in this paper. Such a mode analysis is a complex problem, since the calculated energies show considerable sensitivity to the model

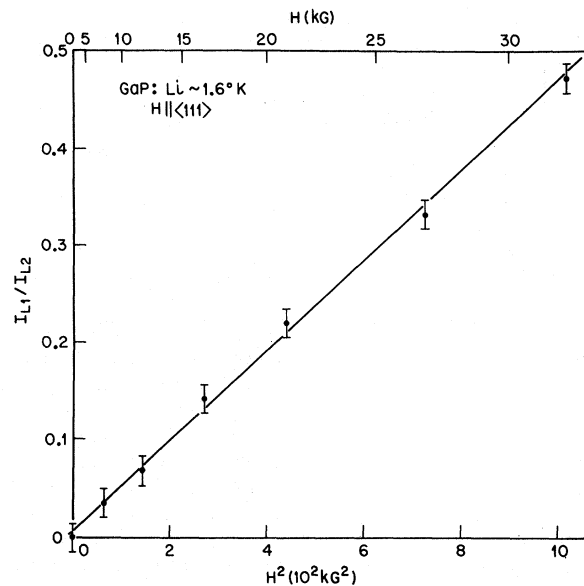


FIG. 8. The dependence of the ratio of intensities of the  $Li_{L1}^0$  and  $Li_{L2}^0$  no-phonon lines on the magnetic field, plotted as  $H^2$  for  $\vec{H} \parallel \langle 111 \rangle$ .

adopted to represent the motion of the ions and the surrounding GaP lattice. Some striking model-insensitive features emerge, however,<sup>31</sup> which are conveniently discussed in terms of the simple model in Fig. 9. Only three force constants  $k_1$ ,  $k_2$ , and  $k_3$  are then needed to describe the basic local motion of the Li-Li-O associate. Isolated Li on a Ga site with unaltered force constants has a local-mode energy of  $\sim 110$  meV. An approximately threefold reduction of the effective force constant on the  $\text{Li}_{\text{Ga}}$  atom is necessary to move this energy into the range of those listed in Table I, using the model in Fig. 9. This large force constant reduction is not surprising, in view of the small size of the Li-Li-O center compared with the Ga-P site it occupies (Sec. III B), and is consistent with the local (in-band resonance) mode observed for Cd-O.<sup>3, 4, 26</sup>

The energy shifts induced by isotopic substitutions (Table II) will be examined in detail, since they provide vital evidence for the Li-Li-O model as we have seen in Sec. III A. The shift  $\Delta\hbar\omega$  in energy of a given local mode due to a change  $\Delta M$  in an ion of mass  $M$ , assuming the force constants to be independent of  $\Delta M$ , is given by

$$\Delta\hbar\omega = \frac{1}{2} \hbar\omega (\Delta M/M) f_{\text{KE}}. \quad (5)$$

Here,  $f_{\text{KE}}$  is the fractional kinetic energy of the mode associated with motion of the given ion. Large values of  $f_{\text{KE}}$  occur only for the true local modes [ $\hbar\omega \gtrsim \hbar\omega(\text{LO}(\Gamma))$ ]. This is expected, since the gap modes are less localized from the surrounding GaP lattice<sup>21</sup> and the in-band resonance mode en-

ergies are strongly pinned by the structure in the density of states of the normal modes of the GaP lattice.<sup>32</sup>

Two local modes are expected for the internal motion of the Li-Li-O center (Fig. 9). Most of the kinetic energy in mode A involves motion of the Li ions, while  $f_{\text{KE}}^0 > f_{\text{KE}}^1$  for mode B. Thus, we tentatively identify mode A with mode L7 in Fig. 2 and Tables I and II. For a particular set of force constants, the energy of mode A is calculated to be  $\sim 59$  meV,<sup>31</sup> cf. 58 meV for L7 in Table I. At the same time a gap mode appears at 31 meV, compared with 36 meV for the experimental energy of the prominent gap mode L1 (Table I). In addition, the predicted energy of local mode B is 82 meV. No local modes are observed experimentally above  $\hbar\omega_{L7}$ . The only other true local mode observed is L6, only  $\sim 0.3$  meV above  $\hbar\omega_{\text{LO}(\Gamma)}$  (Table I). There is no way of reducing  $\hbar\omega_B$  below  $\hbar\omega_A$  with the simple model shown in Fig. 9. In particular, attempts to reduce  $\hbar\omega_B$  by adjusting  $k_3$ , so as to leave  $\hbar\omega_A$  unaltered, will widen the disagreement between experiment and theory for the gap mode. It seems necessary to presuppose that mode B is not seen in the luminescence sideband spectrum, as a result of a low coupling coefficient to the optical transition. The weak low-energy local mode L6 may well involve a set of eigenfunctions which occur in the exact three-dimensional situation, but which have no place in the model in Fig. 9. Alternatively, it may be that a much more complicated force-constant model is needed; in particular it may be necessary to include explicitly the direct coupling between the Li ions and the surrounding GaP lattice. Such models contain too many free parameters to be worthwhile.

Important information is obtained from the properties of the two *extra* local modes present when the  $\text{Li}^6$  and  $\text{Li}^7$  isotopes have comparable concentrations [Fig. 2(c)]. We have already noted in Sec. III A the qualitative result that the presence of *two* extra modes *proves* that there are at least two inequivalently bonded Li atoms in the Li-Li-O complex. Were this not so, only one extra mode would occur, midway between those observed for pure  $\text{Li}^6$  and pure  $\text{Li}^7$ , if the force constants are independent of the isotope mass. From the two isotope shifts observed for  $\text{Li}^{6,7}$ ,  $\Delta\hbar\omega = 1.0$  and 3.3 meV, the  $f_{\text{KE}}$  associated with the two Li atoms can be calculated, and are approximately 0.80 and 0.24. These  $f_{\text{KE}}$  values, together with that for O given in Table II for this (L7) local mode (0.08) sum to 1.0, as near as can be determined from the experimental data. This mode is highly localized, therefore. The intensity ratio of the outer pair of L7 local modes in Fig. 2(c) indicates that the concentration of  $\text{Li}^7 > \text{Li}^6$  in the Li diffusion source used.<sup>33</sup> The fact that the inner pair of local modes

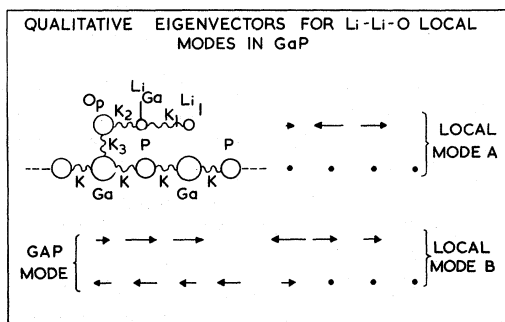


FIG. 9. A linear chain ball and spring model for the local modes of Li-Li-O in GaP, arranged so that only nearest-neighbor forces appear. A minimum of three force constants is required for the Li-Li-O center and its coupling to the lattice, since experiment indicates that the two Li atoms are bonded inequivalently. The arrows represent, on a purely qualitative basis, the eigenvectors for the three basic forms of motion indicated, dots indicating no motion of the corresponding atoms in the ball and spring drawing. Large reductions in the internal force constants  $k_1$  and  $k_2$ , compared with  $k_3$ , are required to match the calculated frequencies with experiment (see text).

for the mixed complex  $\text{Li}^{6,7}\text{-Li}^{7,6}\text{-O}$  also has different intensities suggests that the *form* of the vibrational motion is influenced by these large (14%) changes in isotopic mass. For example the mean length of the Li-O bonds will be significantly different for  $\text{Li}^6\text{-O}$  and  $\text{Li}^7\text{-O}$ , and the electron-phonon coupling constant may be very sensitive to this parameter. We may assume that the electronic transition is coupled directly to the motion of O, since the model in Sec. III B indicates that the exciton is bound through the interaction of the electron with the screened O donor. Then, observation of an O-induced isotopic shift in the no-phonon transition energy [Fig. 2(a)] shows that the force constant which couples the Li-Li-O center to the surrounding GaP lattice is sensitive to the O mass as well as to the presence of the tightly bound electron. This assumption is consistent with the sensitivity of the *form* of the optical phonon replicas near 2.04 eV to the mass of the O atom [Figs. 1(a) and 2(a)]. One might speculate that the more tightly bound Li atom is the one on the Ga lattice site, rather than the Li atom in the P-like interstitial site (Fig. 9). Such speculation can be tested only by rather detailed examination of the vibrational motion, with force-constant models chosen appropriately to simplify the number of independent parameters. This analysis is outside the scope of the present paper.

#### E. Absorption of Li-Li-O Center

The absorption spectrum due to the photocreation of an exciton on the Li-Li-O center is an approximate mirror image of the red luminescence spectrum about the no-phonon lines. The presence of three no-phonon lines in absorption has already been discussed in Sec. III B. The two higher-energy lines  $\text{Li}_{L_{3,4}}^0$  are poorly resolved, as in luminescence, producing a resultant roughly twice as broad as  $\text{Li}_{L_2}^0$ . The precise shape of the phonon wing is hard to determine from the transmission spectrum in Fig. 4(b), and the finer details of the structure superposed upon it cannot be clearly seen because of their weakness. Better defined phonon sidebands have been obtained in excitation spectra of the Li-Li-O luminescence, and data from these spectra have been included in Table I. It is clear that the strong gap modes resolved have slightly lower energy than in luminescence, whereas the phonon energies from the other peaks in the absorption sideband are essentially identical to those from the luminescence sideband. The true local modes are not visible in the absorption spectrum in Fig. 4(b) or in the luminescence excitation spectra. The sign of the shift in the no-phonon energy shown in Fig. 2 for the isotopic substitution  $\text{O}^{16}\text{-O}^{18}$  implies that the *average* local-mode energy is greater in the presence of the bound exciton,

i. e., this energy should be larger in the low-temperature phonon sideband in optical absorption compared with luminescence. The phonon energy associated with the  $\text{Li}_{L_2}^1$  replica in the absorption spectrum increases by  $\sim 0.5$  meV on the isotopic substitution  $\text{Li}^7\text{-Li}^6$ , like the shift observed in luminescence (Table II), and rather large changes in relative strength of the gap modes occur in the absorption spectrum.

The concentration of Li-Li-O centers can be determined from the absorption cross section of the  $\text{Li}_{L_2}^0$  no-phonon line and the form of the luminescence spectrum if the relevant transition oscillator strength  $f_{L_2}$  is known. The latter quantity may be determined from the luminescence lifetime  $\tau$ , assuming detailed balance in the absence of Auger or other nonradiative decay of the bound exciton.<sup>34</sup> The lifetime  $\tau$  is temperature dependent because of thermalization of the  $\text{Li}_{L_2}^0$  line into  $\text{Li}_{L_1}^0$  at low temperatures. At 4.2 °K,  $\tau = 720$  nsec, while  $\tau = 200$  nsec at 20.6 °K. The latter lifetime is probably about 3 times the lifetime of the allowed  $L_2$  transition in view of experience with similar exciton transitions.<sup>34,35</sup> Then

$$f_{L_2} = \frac{1.5\lambda^2\tau_{L_2} g_i}{n g_f} . \quad (6)$$

Here  $\lambda$  is the transition wavelength,  $n$  is the refractive index, and  $g_i, g_f$  are the degeneracies of the initial and final states. For transition  $\text{Li}_{L_2}^0\lambda = 6100$  Å,  $n = 3.35$ ,  $g_i = 1$ , and  $g_f = 2$ . Thus  $f_{L_2} = 0.051$  for  $\tau_{L_2} = 7 \times 10^{-8}$  sec, similar to the values for the N<sup>34</sup> and Cd-O<sup>35</sup> isoelectronic traps.

For a Gaussian line, the concentration of impurity centers,  $N_{\text{Li-Li-O}}$  is given by<sup>36</sup>

$$N_{\text{Li-Li-O}} = 9.6 \times 10^{15} n (\alpha_{\text{max}} \Gamma)_{L_2} / f_{L_2} \text{ cm}^{-3} . \quad (7)$$

In this equation  $(\alpha_{\text{max}} \Gamma)_{L_2}$  represents the total strength of the transition, including the phonon sideband. It may be estimated from the area under the  $\text{Li}_{L_2}^0$  line [in  $\text{cm}^{-1}\text{eV}$  for Eq. (7)], taking account of the ratio of the total area under the  $L_2$  luminescence spectrum to the area under the luminescence line  $\text{Li}_{L_2}^0$ . This ratio was measured at 4.2 °K, where the contributions of  $\text{Li}_{L_1}$  and  $\text{Li}_{L_{3,4}}$  to the luminescence sideband are negligible, and is 23.5. Then  $N_{\text{Li-Li-O}} = 1.4 (\alpha_{\text{max}} \Gamma)_{\text{Li}_{L_2}^0} \times 10^{17} \text{ cm}^{-3}$  where  $(\alpha_{\text{max}} \Gamma)_{\text{Li}_{L_2}^0}$  is the area under the  $\text{Li}_{L_2}^0$  line in  $\text{cm}^{-1}\text{meV}$ . For typical needles grown at 950 °C by the wet  $\text{H}_2$  vapor transport method,  $(\alpha_{\text{max}} \Gamma)_{\text{Li}_{L_2}^0} \approx 0.3 \text{ cm}^{-1}\text{meV}$ , so that  $N_{\text{Li-Li-O}} \sim 4 \times 10^{16} \text{ cm}^{-3}$  for standard conditions of Li diffusion (700 °C/60 min). Assuming that the vapor-growth conditions are such that the GaP is saturated with O at 950 °C, with the  $\text{P}_2$  pressure close to the decomposition pressure of GaP, then  $N_{\text{O}}$  can be estimated from Foster and Scardefield's<sup>37</sup> 1050 °C distribution coefficient for O, and is  $\sim 4 \times 10^{16} \text{ cm}^{-3}$ .<sup>38</sup> It is difficult to make

precise comparisons between  $N_{\text{Li-Li-O}}$  and  $N_{\text{O}}$  because of the assumptions leading to Eq. (7) (neglect of the local-field correction, for this relatively tightly bound state) and in the estimate of  $N_{\text{O}}$ . In addition, considerable variations in the quantity  $(\alpha_{\text{max}}\Gamma)_{\text{Li}_2^0}$  have been observed (factor of 5) after separate Li diffusions by the first method described in Sec. IIA into crystals obtained from the same GaP growth run. The value used above is the maximum observed after Li diffusion of 60 min at 700 °C in vapor-grown needles. It is believed that this variation is a defect of the diffusion method and that more reproducible Li-Li-O absorption strengths might be obtained from crystals Li diffused by the Pell method (Sec. IIA). However, the essential point is that these two concentrations are of the same order even though no attempt has been made to optimize  $N_{\text{Li-Li-O}}$ , for example, by annealing at lower temperature after the 700 °C Li diffusion. It will be argued in Sec. III F that this relative parity of  $N_{\text{Li-Li-O}}$  and  $N_{\text{O}}$  proves that Li diffusion provides a very useful technique for labeling a specific major proportion of the substitutional O in GaP, so that the concentration of O in this specific form ( $V_{\text{Ga}}\text{-O}_\text{P}$  pairs) may be estimated very readily.

#### F. Defect Chemistry of Li-Li-O Center

It was noted in Sec. IIA that O-doped Czochralski-grown (LEC) GaP did not show the red luminescence characteristic of the Li-Li-O center after the standard Li diffusion (700 °C/60 min). Before the Li diffusion, these crystals were as received from the LEC puller, where they had been quenched from 1200–1300 °C after completion of the pulling operation. On the other hand, O-doped GaP grown at ~1100 °C from Ga solution, or quenched from 1100 °C after growth from a Ga-rich pulled melt, and O-doped needles grown from the vapor at ~950 °C, invariably showed strong Li-Li-O luminescence. In addition it was noted that strong red Li-Li-O luminescence occurred at Li diffusion temperatures at least as low as 400 °C, from those regions of the vapor- or solution-grown crystals which were physically in contact with the Li metal. These observations suggest two things. First, it is very unlikely that the  $V_{\text{Ga}}\text{-O}_\text{P}$  pairs, which must exist as a preliminary stage in the formation of the  $\text{Li}_\text{I}\text{-Li}_{\text{Ga}}\text{-O}_\text{P}$  center, are created during the minimal conditions of Li diffusion we used (400 °C/60 min). We presume the  $V_{\text{Ga}}\text{-O}_\text{P}$  associates already exist, and the  $\text{Li}_\text{I}\text{-Li}_{\text{Ga}}\text{-O}_\text{P}$  complexes are formed when the Li diffuses to the  $V_{\text{Ga}}\text{-O}_\text{P}$  pairs by an interstitial mechanism.<sup>39</sup> Second, if the  $V_{\text{Ga}}\text{-O}_\text{P}$  pairs have a heat of formation substantially higher than the  $\text{Zn}_{\text{Ga}}\text{-O}_\text{P}$  pairs, it is possible that they associate in the temperature range 900–1000 °C, where migration of  $V_{\text{Ga}}$  is plausible,<sup>40</sup> while the  $\text{Zn}_{\text{Ga}}\text{-O}_\text{P}$

pairs are known to become thermally dissociated in this temperature range.<sup>41</sup> If we further presume that the  $V_{\text{Ga}}\text{-O}_\text{P}$  pairs become thermally dissociated above ~1200 °C, the set of observations outlined above immediately becomes comprehensible. Further extensive and careful studies are evidently required to establish more precise limits to the temperature ranges of association and to evaluate the defect kinetics quantitatively.

If the model outlined above is correct, it is clear that Li diffusion forms a convenient way of labeling an elusive type of crystal defect, namely, the vacancy. The optical spectroscopy of Li-diffused GaP could be a valuable tool in the study of the properties of Ga vacancies, directly in the  $V_{\text{Ga}}\text{-O}_\text{P}$  associates and indirectly in other forms (e.g., isolated  $V_{\text{Ga}}$ ). The efficient highly structured luminescence of the Li-Li-O associate may also be utilized for other chemical studies. For example, attempts have been made to dope LEC GaP with  $\text{O}^{18}$ , introduced in a  $\text{Ga}_2\text{O}_3$  dopant charge. Small pieces of the resultant ingot were annealed at 975 °C and diffused with  $\text{Li}^7$  at 700 °C. Quite intense Li-Li-O exciton luminescence resulted, and it was clear from the sharp line  $\text{Li}_2^0$  [Fig. 2(a)] that the  $\text{O}^{18}/\text{O}^{16}$  isotope ratio was at most a few percent. Evidently, there is appreciable exchange of O between the  $\text{GaP} + \text{Ga}_2\text{O}_3$  charge and the  $\text{B}_2\text{O}_3$  encapsulation during the pulling operation. This result is of consequence in the study of local modes through infrared absorption, since it was thought that the lack of an O isotope shift from these crystals might rule out the participation of O.<sup>42</sup> It also has important general implications for attempts to control the O concentration in the LEC crystals.

The discovery that a large proportion of the substitutional O may exist in the  $V_{\text{Ga}}\text{-O}_\text{P}$  associates (Sec III E) is also highly significant. This proportion of the O could be excluded from the formation of  $\text{Zn}_{\text{Ga}}\text{-O}_\text{P}$  pairs, which are essential for the red luminescence used in red GaP diodes. This is so because the Zn diffuses towards the O by an interstitial-substitutional mechanism, driven by the strong Coulomb attraction between  $\text{Zn}_{\text{Ga}}$  and  $\text{O}_\text{P}$ .<sup>43, 44</sup> However, the associate  $V_{\text{Ga}}\text{-O}_\text{P}$  is a double *acceptor*, and exhibits Coulomb *repulsion* towards  $\text{Zn}_{\text{Ga}}$ . In addition, the  $V_{\text{Ga}}\text{-O}_\text{P}$  double acceptor may be positively harmful by inducing strong Auger recombinations for holes.<sup>45</sup> These considerations suggest that the red (and green) electroluminescence efficiency of GaP LPE (liquid-phase epitaxy) layers might be improved by an anneal at 1200–1300 °C prior to a ~600 °C anneal to form  $\text{Zn}_{\text{Ga}}\text{-O}_\text{P}$  associates (for red luminescence). Such annealing treatment would have to be performed in the high-pressure puller to avoid dissociation of the GaP. Unfortunately, the potential gain is rather small (less than 2 times the increase of efficiency) and may well be outweighed

by unanticipated deleterious effects of this rather drastic annealing treatment.

#### G. Temperature Quenching of Li-Li-O Luminescence

We have seen that the red Li-Li-O photoluminescence is very efficient at low temperatures, as expected for exciton recombination at an isoelectronic trap. The mean energy of this luminescence exceeds that of the red Zn-O luminescence by  $\sim 0.19$  eV at low temperatures, and its luminous equivalent is therefore significantly higher. Unfortunately, we have not been able to produce efficient Li-Li-O luminescence at room temperature. The Li-Li-O photoluminescence usually quenches very rapidly with increasing temperature (Fig. 10) compared with the red Zn-O luminescence.<sup>46</sup> The 300 °K red electroluminescence efficiency of ZnO- and CdO-doped light emitting diodes (LEDs) was greatly reduced by Li diffusion, although the red Li-Li-O band could be seen at low temperatures ( $\sim 78$  °K), where it also quenched the red Zn-O and Cd-O luminescence. The electrical properties of the Li-diffused diodes showed evidence of strong compensation of the  $p$  region.

Optimum high-temperature performance of the Li-Li-O radiative recombination center is expected in  $p$ -type material, since the electron is the tightly bound particle. The situation is similar to the behavior of the isoelectronic trap O in ZnTe,<sup>34</sup> with the additional factor that the concentration of substitutional O should be significantly greater in  $p$ -type GaP.<sup>47</sup> However, diffusion with Li drastically reduces the concentration of neutral acceptors, i. e., of free holes at high temperatures. This reduction lengthens the total (radiative + Auger) lifetime of electrons on Li-Li-O centers. It is always necessary to consider the presence of a nonradiative shunt recombination path for minority carriers in GaP.<sup>48</sup> The lengthened electron recombination time on the Li-Li-O centers reduces the branching ratio of the recombination rates through the Li-Li-O center and the shunt path if the total Li-Li-O recombination time is long compared with the electron thermalization time out of the Li-Li-O traps. This condition is easily realized at 300 °K, since the electron binding energy is only  $\sim 200$  meV, significantly less than for the Zn-O associate.<sup>49</sup> The lengthened recombination time also accentuates the luminescence saturation effect, which is a characteristic of red Zn-O luminescence in GaP. These considerations can readily account for the relatively rapid temperature quenching of the red Li-Li-O luminescence. It would appear that these undesirable effects of the close compensation resulting from the Li diffusion can only be circumvented by a Zn in-diffusion subsequent to the Li diffusion. However, this would have to be carried out at  $\sim 850$  °C,<sup>50</sup> a much higher temperature than for the

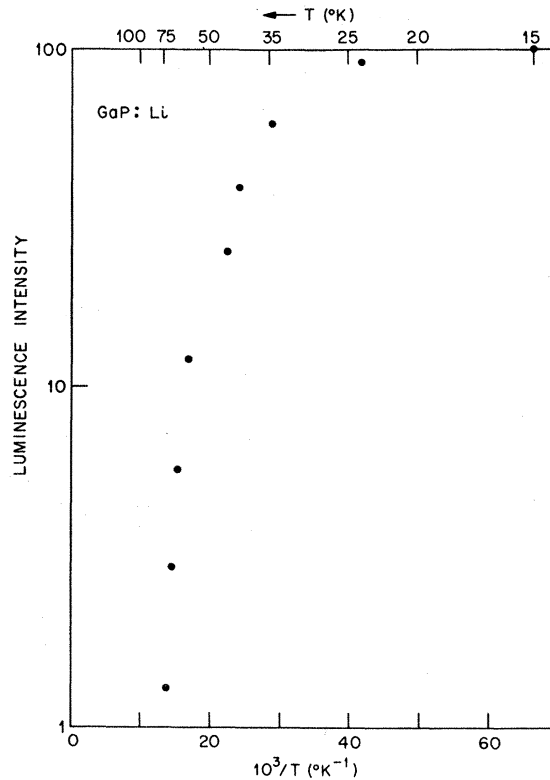


FIG. 10. The temperature dependence of the Li-Li-O exciton luminescence intensity for low-level optical excitation in a compensated crystal.

Li diffusion. It is clear that this is not an attractive procedure for the construction of an LED.

The photoluminescence spectrum of O-doped Li-diffused GaP changes drastically near 50 °K. Below this temperature the red Li-Li-O spectrum shown in Fig. 4(a) usually predominates, except in unannealed LEC material as discussed in Secs. II A and III F. Above  $\sim 50$  °K, a broad featureless lower-energy band peaking near 1.75 eV sometimes becomes predominant (Fig. 11). This band may be seen as a low-energy shoulder on the red Li-Li-O band at temperatures  $\lesssim 20$  °K. However, it is not invariably present at 65 °K. Some Li-diffused vapor-grown GaP and most Li-diffused solution-grown material show only weak low-energy shoulders to the red Li-Li-O band even at 65 °K, and often the dominant low-energy band does not peak precisely at 1.75 eV. The origin of the 1.75-eV band is therefore unclear. It is evidently not solely due to Li, although it was not a prominent feature of the 65 °K spectrum of the vapor-grown crystals used for Fig. 11 before Li diffusion. The 1.75-eV band intensity is not included in the ordinate of Fig. 10. However, the absolute intensity in this band is also sharply reduced above  $\sim 100$  °K. This band is of no interest in the design of an efficient

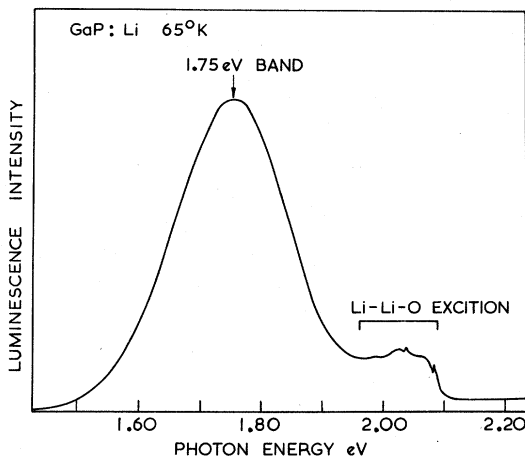


FIG. 11. Photoluminescence spectrum from Li-diffused GaP at 65°K, showing a relatively strong broad unidentified band centered on  $\sim 1.75$  eV.

red GaP LED because its luminous equivalent is less than for the red Zn-O luminescence.

#### IV. SUMMARY

The bright red low-temperature photoluminescence characteristic of Li-diffused GaP has been studied in detail. The spectrum is due to the recombination of excitons bound by  $\sim 0.24$  eV to an axial defect. Isotope shifts in the no-phonon lines and in many local-mode phonon replicas prove the involvement of Li and O in this defect. A model is presented, whereby a GaP atom pair is replaced by  $\text{Li}_I\text{-Li}_{\text{Ga}}\text{-O}_P$  forming an isoelectronic compound substitution. This model is the simplest center consistent with the experimental data on transition lifetime, energy, and radiative efficiency, and with the Li isotope effects on the local modes, and has  $\langle 111 \rangle$  symmetry as required from Zeeman analysis of the lowest-energy no-phonon line. The success of this simple model in accounting for a wide variety of detailed experimental data is strong proof of its validity. The zero-field and Zeeman properties of the no-phonon lines are qualitatively similar to those previously reported for the Cd-O associate in GaP, and the  $g$  values are essentially identical. However, only the two lowest out of the four no-phonon lines expected to be visible were seen for Cd-O. The no-phonon line pattern for Li-Li-O is approximately described by a simple model in which two basic splittings occur due to  $J$ - $J$  coupling and the uniaxial crystal field of the Li-Li-O associate. The crystal-field *splitting* is only  $\sim 3$  times the  $J$ - $J$  splitting, yet the observed and calculated crystal-field *mixing* of the  $J=1$  and  $J=2$  states is close to the limit for infinitely large field.

A study of the preparation conditions for the

Li-Li-O luminescence spectrum in GaP crystals grown under different conditions has been rewarding. First, the fact that the spectrum can be seen strongly in crystals diffused with Li at temperatures at least as low as 400 °C suggests that the  $V_{\text{Ga}}\text{-O}_P$  pairs, which are a necessary stage in the formation of the  $\text{Li}_I\text{-Li}_{\text{Ga}}\text{-O}_P$  associate, are present in the crystals *before* Li diffusion. Typical concentrations of the  $V_{\text{Ga}}\text{-O}_P$  pairs, established in vapor-grown needles from optical absorption using an oscillator strength determined from the luminescence time decay, are an appreciable fraction ( $\sim \frac{1}{4}$ ) of the total concentration of substitutional O. Second, the Li-Li-O luminescence can only be obtained from LEC crystals pulled from a high-temperature stoichiometric melt, even when O-doped, after the resulting ingot material is annealed at  $\sim 1000$  °C. Since  $[V_{\text{Ga}}]$  increases rapidly with growth temperature, this effect cannot be simply due to changes in this concentration for the differently prepared crystals. It is postulated that the heat of association of the  $V_{\text{Ga}}\text{-O}_P$  pair is such that these pairs are not stable at 1200–1300 °C, temperatures from which the LEC crystals are quenched after growth, but are stable at 950–1200 °C, and especially at the lower end of this growth temperature range for wet  $\text{H}_2$  vapor growth, growth from Ga solution at atmospheric pressure or from strongly Ga-rich melts in the LEC puller. Thus, if the model is valid, Li diffusion provides an easy and versatile method whereby the concentration of  $V_{\text{Ga}}$  in a particular form ( $V_{\text{Ga}}\text{-O}_P$  associates) can be determined from optical absorption alone. This is significant, since *definitive* experimental information on the behavior of vacancies in III-V compounds has not been available previously. In addition, Li diffusion forms an extremely convenient tracer technique for the state of O in GaP. For example, the relative abundance of  $\text{O}^{18}$  and  $\text{O}^{16}$  can be determined simply and accurately (readily to a few %) from the relative intensities of the two well-resolved components of the strong  $\text{Li}_{L2}^0$  no-phonon luminescence which occur in the presence of these O isotopes. This measurement technique can be combined with  $\text{O}^{18}$  doping to study the degree of control of O doping in GaP crystals grown by various methods. Preliminary results suggest that  $\text{O}^{18}$  doping of LEC crystals grown from a stoichiometric melt, through the addition of  $\text{Ga}_2\text{O}_3$  to the growth charge, is not straightforward and probably inefficient. It is clear that further more systematic and extensive studies of the effects of growth, post growth annealing, and Li diffusion conditions on the intensities of the red Li-Li-O luminescence and absorption will yield much quantitative information about properties of GaP which have strong relevance to the preparation of efficient light emitting diodes from this material.

## ACKNOWLEDGMENTS

The author is indebted to the following for substantial assistance in connection with this paper: A. S. Barker, Jr. for the preliminary results of his linear-chain-model calculations on the local modes of the Li-Li-O associate, discussed in Sec. III D; R. Berman for supplying many LEC GaP crystals Li diffused by the Pell technique (Sec. II A); R. A. Logan for the electroluminescence data discussed in Sec. III G; and C. D. Thurmond

for the estimate of [O] quoted in Sec. III E for vapor-grown GaP. Generous advice concerning the  $J$ - $J$  coupling model, the magneto-optical properties, and the local modes of the Li-Li-O isoelectronic trap was provided by J. J. Hopfield, R. A. Faulkner, and Jane van W. Morgan. Almost all the Li diffusions by the first technique described in Sec. II A and all the optical transmission measurements were expertly carried out by G. Kaminsky. Facilities for the Zeeman experiments were generously provided by J. L. Merz.

\*Present address: Royal Radar Establishment, Malvern, Worcestershire, England.

<sup>1</sup>D. G. Thomas and J. J. Hopfield, *Phys. Rev.* **150**, 680 (1966).

<sup>2</sup>P. J. Dean, in *Applied Solid State Science*, edited by R. Wolfe (Academic, New York, 1970), Vol. 1, p. 1.

<sup>3</sup>T. N. Morgan, B. Welber, and R. N. Bhargava, *Phys. Rev.* **166**, 751 (1968).

<sup>4</sup>C. H. Henry, P. J. Dean, and J. D. Cuthbert, *Phys. Rev.* **166**, 754 (1968).

<sup>5</sup>This point went unrecognized in a preliminary report of this work, in which the center was described as  $\text{Li}_I\text{-Li}_{\text{Ca}}\text{O}_P$ , by P. J. Dean, *Bull. Am. Phys. Soc.* **16**, 328 (1971).

<sup>6</sup>The  $\text{Li}_2\text{O}$  molecule may be represented as  $\text{Li-O-Li}$ . The linear geometry of this gas molecule seems to be established by the molecular-beam studies of L. Wharton, R. A. Berg, and W. Klemperer, *J. Chem. Phys.* **39**, 2023 (1963).

<sup>7</sup>E. W. Williams, *Phys. Rev.* **163**, 922 (1968).

<sup>8</sup>S. J. Bass and P. E. Oliver, *J. Cryst. Growth* **3**, 4, 286 (1968).

<sup>9</sup>G. A. Wolff, R. A. Herbert, and J. P. Broder, *Phys. Rev.* **100**, 1144 (1955); L. M. Foster, T. S. Plaskett, and J. E. Scardefield, *IBM J. Res. Develop.* **10**, 114 (1966).

<sup>10</sup>C. J. Frosch, *Proceedings of the International Conference on Crystal Growth, Boston*, 1966 (Pergamon, New York, 1967), p. 305.

<sup>11</sup>C. S. Fuller and K. B. Wolfstirn, *J. Appl. Phys.* **33**, 2507 (1962).

<sup>12</sup>E. M. Pell, *J. Phys. Chem. Solids* **3**, 77 (1957).

<sup>13</sup>R. Berman (private communication).

<sup>14</sup>P. J. Dean and C. H. Henry, *Phys. Rev.* **176**, 928 (1968).

<sup>15</sup>H. Reiss and C. S. Fuller, *J. Metals* **8**, 276 (1956).

<sup>16</sup>W. Hayes, *Phys. Rev.* **138**, A1227 (1965).

<sup>17</sup>P. J. Dean, R. A. Faulkner, S. Kimura, and M. Ilegems, *Phys. Rev. B* (to be published).

<sup>18</sup>J. L. Yarnell, J. L. Warren, R. G. Wenzel, and P. J. Dean, *Neutron Inelastic Scattering* (IAEA, Vienna, 1968), p. 301.

<sup>19</sup>This is true even at 1.6°K, where  $\Delta E \approx 7kT$ .

<sup>20</sup>R. E. Dietz, D. G. Thomas, and J. J. Hopfield, *Phys. Rev. Letters* **8**, 391 (1962).

<sup>21</sup>L. Genzel, in *Optical Properties of Solids*, edited by S. Nudelman and S. S. Mitra (Plenum, New York, 1969), Chap. 15.

<sup>22</sup>According to a one-phonon density of states constructed by J. L. Warren from a multiparameter fit to the phonon-dispersion curves determined in Ref. 18, this gap extends from ~31 to ~40 meV.

<sup>23</sup>P. J. Dean, C. H. Henry, and C. J. Frosch, *Phys. Rev.* **168**, 812 (1968).

<sup>24</sup>At 4.2°K the red Li-Li-O luminescence is of comparable quantum efficiency to that from other isoelectronic traps in GaP, such as Bi and N. However, temperature quenching of the Li-Li-O luminescence is strong above ~50°K (Sec. III G).

<sup>25</sup>D. F. Nelson, J. D. Cuthbert, P. J. Dean, and D. G. Thomas, *Phys. Rev. Letters* **17**, 1262 (1966).

<sup>26</sup>C. H. Henry, P. J. Dean, D. G. Thomas, and J. J. Hopfield, in *Proceedings of the International Conference on Localized Excitation in Solids*, edited by R. F. Wallis (Plenum, New York, 1968), p. 267.

<sup>27</sup>The  $s$ -like character of electrons bound to  $P$ -site donors in GaP was first postulated by D. G. Thomas, M. Gershenzon, and J. J. Hopfield, *Phys. Rev.* **131**, 2397 (1963), and explicitly justified by T. N. Morgan, *Phys. Rev. Letters* **21**, 819 (1968).

<sup>28</sup>P. J. Dean and R. A. Faulkner, *Phys. Rev.* **185**, 1064 (1969).

<sup>29</sup>Jane van W. Morgan and T. N. Morgan, *Phys. Rev. B* **1**, 739 (1970).

<sup>30</sup>J. L. Merz, R. A. Faulkner, and P. J. Dean, *Phys. Rev.* **188**, 1228 (1969).

<sup>31</sup>A. S. Barker, Jr. (private communication).

<sup>32</sup>P. G. Dawber and R. J. Elliott, *Proc. Phys. Soc. (London)* **A287**, 64 (1965).

<sup>33</sup>Mass spectrographic analysis gives a  $\text{Li}^6/\text{Li}^7$  ratio of  $0.69 \pm 0.07$ .

<sup>34</sup>J. D. Cuthbert and D. G. Thomas, *Phys. Rev.* **154**, 763 (1967).

<sup>35</sup>J. D. Cuthbert, C. H. Henry, and P. J. Dean, *Phys. Rev.* **170**, 739 (1968).

<sup>36</sup>D. L. Dexter, *Phys. Rev.* **101**, 48 (1956).

<sup>37</sup>L. M. Foster and J. E. Scardefield, *J. Electrochem. Soc.* **116**, 494 (1969).

<sup>38</sup>C. D. Thurmond (private communication).

<sup>39</sup>Lithium diffuses by an interstitial (rather than an interstitial-substitutional) mechanism in Si; G. S. Fuller and J. C. Severiens, *Phys. Rev.* **95**, 21 (1954), and also in GaAs; C. S. Fuller and K. B. Wolfstirn, *ibid.* **33**, 2507 (1963), even though interstitial Li reacts with  $V_{\text{Ga}}$  to form substitutional Li acceptors at the end of the diffusion process in GaAs. Note that Li does not compensate heavily  $n$ -type GaP (Sec. II A), a sharp distinction from its behavior in GaAs.

<sup>40</sup>It is also possible that the O atoms can diffuse at ~1000°C over the small distances needed for  $V_{\text{Ga}}\text{-O}_P$  association from an initially random relative distribution of  $V_{\text{Ga}}$  and  $\text{O}_P$ . Hayes (Ref. 16) has suggested that  $V_{\text{Ga}}$  may be preferentially created adjacent to As-site donors



in GaAs, in material initially diffused at rather high temperatures ( $\sim 800^\circ\text{C}$ ). There is no clear evidence for such an effect for  $V_{\text{Ga}}-O_{\text{P}}$  in GaP from the present work. However, more detailed electrical and optical studies are required to clarify this point.

<sup>41</sup>C. S. Fuller and K. B. Wolfstirn [J. Appl. Phys. **34**, 1914 (1963)] have found evidence for a very large heat of association of  $V_{\text{Ga}}\text{Te}_{\text{As}}$  pairs in GaAs.

<sup>42</sup>R. Berman and A. S. Barker, Jr. (private communication).

<sup>43</sup>A. Onton and M. R. Lorenz, Appl. Phys. Letters **12**, 115 (1968).

<sup>44</sup>J. Wiley, J. Phys. Chem. Solids (to be published).

<sup>45</sup>This is so because binding characteristic of a double acceptor may greatly increase the Auger transition rate through the strong hole-hole overlap and ease of momentum

conservation for the ejected hole (see Ref. 17).

<sup>46</sup>M. Gershenson and R. M. Mikulyak, Appl. Phys. Letters **8**, 245 (1966).

<sup>47</sup>H. Reiss, C. S. Fuller, and F. J. Morin, Bell System Tech. J. **35**, 535 (1956).

<sup>48</sup>W. Rosenzweig, W. H. Hackett, Jr., and J. S. Jayson, J. Appl. Phys. **40**, 4477 (1969).

<sup>49</sup>We have seen that the low-temperature electron binding energy at Li-Li-O is 210 meV [=  $(E_{\text{bx}} + E_x - E_h)$ ], where  $E_x$  is the internal binding energy of the exciton and  $E_h$  is the binding energy of the hole to the electron on Li-Li-O]. The corresponding energy is  $\sim 300$  meV for the Zn-O trap (Ref. 35).

<sup>50</sup>L. L. Chang and G. L. Pearson, J. Appl. Phys. **35**, 374 (1964).

## Hopping Conductivity in Disordered Systems

Vinay Ambegaokar\*

*Research Institute for Theoretical Physics, University of Helsinki, Finland*

and

B. I. Halperin

*Bell Telephone Laboratories, Murray Hill, New Jersey 07974*

and

J. S. Langer†

*Carnegie-Mellon University, Pittsburgh, Pennsylvania 15213*

(Received 14 May 1971)

By considering a model in which charge is transported via phonon-induced tunneling of electrons between localized states which are randomly distributed in energy and position, Mott has obtained an electrical conductivity of the form  $\sigma \propto \exp[-(\lambda\alpha^3/\rho_0 kT)^{1/4}]$ . Here  $T$  is the temperature of the system,  $\rho_0$  is the density of states at the Fermi level,  $\lambda$  is a dimensionless constant, and  $\alpha^{-1}$  is the distance for exponential decay of the wave functions. We rederive these results, relating  $\lambda$  to the critical density of a certain dimensionless percolation problem, and we estimate  $\lambda$  to be approximately 16. The applicability of the model to experimental observations on amorphous Ge, Si, and C is discussed.

### I. INTRODUCTION

The dc conductivity of amorphous germanium, in the temperature range  $60^\circ\text{K} \leq T \leq 300^\circ\text{K}$ , has been found to be consistent with the law<sup>1-5</sup>

$$\sigma(T) \propto \exp[-(T_0/T)^{1/4}], \quad (1.1)$$

where  $T_0 \cong 7 \times 10^7$  K. Similar temperature dependences have been found in amorphous silicon and carbon,<sup>3, 6, 7</sup> and in vanadium oxide (VO).<sup>8</sup> A temperature dependence of this general form has been predicted by Mott.<sup>9, 10</sup> His ideas are based on a model in which charge is transported by the thermally assisted hopping of electrons between states localized near randomly distributed "traps"—potential fluctuations that can bind electrons. The

temperature  $T_0$  in (1.1) is given by Mott as

$$kT_0 = \lambda \alpha^3 / \rho_0, \quad (1.2)$$

where  $\alpha$  is the coefficient of exponential decay of the localized states,  $\rho_0$  is the density of states at the Fermi level, and  $\lambda$  is a dimensionless constant. Mott's derivation of Eq. (1.1) seems to us to be somewhat unsatisfactory from a statistical point of view. In this paper we present what we feel is a more systematic derivation of the  $T^{-1/4}$  law, starting from Mott's model. Our analysis is rather different from Mott's, however, and seems to us to uncover some important aspects of an extremely interesting problem in statistical physics. In addition, we express the constant  $\lambda$  in terms of the critical density for a certain dimensionless percola-